Applied Catalysis A: General xxx (2015) xxx–xxx

Contents lists available at ScienceDirect

Applied Catalysis A: General

journal homepage: www.elsevier.com/locate/apcata

Reactivity and stability of supported Pd nanoparticles during the liquid-phase and gas-phase decarbonylation of heptanoic acid

Juan A. Lopez-Ruiz[a], Hien N. Pham[b], Abhaya K. Datye[b], Robert J. Davis[a,*]

[a] Department of Chemical Engineering, University of Virginia, Charlottesville, VA 22904-4741, USA
[b] Department of Chemical and Biological Engineering and Center for Microengineered Materials, University of New Mexico, Albuquerque, NM 87131, USA

ARTICLE INFO

Article history:
Received 8 September 2014
Received in revised form 14 January 2015
Accepted 20 January 2015
Available online xxx

Keywords:
Decarbonylation
Deoxygenation
Carboxylic acid
Heptanoic acid
Hexane
Hexene
Pd/C
Pd/SiO_2
Olefin
Paraffin

ABSTRACT

The liquid-phase and gas-phase decarbonylation of heptanoic acid over carbon- and silica-supported Pd nanoparticles was studied in a continuous-flow fixed-bed reactor at 573 K. The liquid-phase turnover frequency (TOF) under steady state conditions (>20 h) was very low at ≈0.00070 s^{-1}, presumably because of deposition of carbonaceous species and in some cases sintering of the metal particles, as revealed by H_2 chemisorption, X-ray diffraction and electron microscopy. The steady state rate was independent of the support composition, synthesis method, Pd loading (1–20 wt%), and acid concentration (0.1–6.6 M). Although the gas-phase reaction also led to deactivation of the supported Pd catalysts, extrapolation of the rate to initial time gave a TOF of ≈0.035 s^{-1} at 573 K. The liquid- and gas-phase reactions at low conversion levels were selective towards the formation of decarbonylation products such as CO and hexenes. Higher conversion levels resulted in the subsequent conversion of the primary decarbonylation products. *Post mortem* analysis of the catalysts revealed that concentrated, liquid-phase heptanoic acid at 573 K severely sintered the Pd nanoparticles supported on carbon but not those supported on silica. The Pd nanoparticles were able to maintain the high dispersion on carbon when exposed to low concentrations of liquid-phase heptanoic acid or gaseous heptanoic acid at 573 K.

1. Introduction

Biomass is an abundant, carbon-neutral alternative resource to fossil fuels for the production of fuels and chemicals. Processing of biomass presents a chemical challenge because it often contains excess oxygen that needs to be removed [1]. Dehydration, ketonization, decarbonylation and decarboxylation comprise a set of transformations collectively regarded as deoxygenation reactions. Organic acids, such as carboxylic acids, are biomass-derived molecules that can be readily converted to hydrocarbons by deoxygenation reactions. As shown in Scheme 1, linear carboxylic acids can be converted into linear olefins and paraffins by decarbonylation and decarboxylation, respectively. Ketonization is also an important reaction for the production of fine chemicals and fuels [2,3] in which two carboxylic acid molecules couple to form a symmetrical ketone, CO_2, and H_2O, as depicted in Scheme 2.

In our previous work, we studied the decarbonylation of heptanoic acid over Pt nanoparticles and reported low α-olefin selectivities because of olefin isomerization and sequential hydrogenation when the reaction was run at modest conversions [4]. At low conversions, however, decarbonylation was the primary reaction path [4]. Whereas Boda et al. [5] and Lugo-José et al. [6,7] also reported that decarbonylation was the main deoxygenation reaction over Pd catalysts, much of the deoxygenation literature [8–22] reports decarboxylation occurs when performing experiments in the presence of dihydrogen and solvent to inhibit catalyst deactivation and maximize the selectivity towards the formation of paraffins [17]. Discriminating between competing reaction paths based solely on the hydrocarbon products that are formed is difficult because alkenes are readily hydrogenated in the presence of H_2 and Pd. Nevertheless, Maier et al. speculated the active site on a Pd catalyst to be a Pd/H complex [23]. Interestingly, quantum chemical studies by Lamb et al. explored a potential mechanistic path to decarboxylate butanoic acid on a model Pd (1 1 1) surface [24], whereas Heyden and co-workers revealed a path to decarbonylate propanoic acid on Pd (1 1 1) [25,26].

Support composition and metal particle size have also been reported to affect the catalyst activity. For example, Lugo-José et al. studied the gas-phase decarbonylation of propanoic acid and

* Corresponding author at: Department of Chemical Engineering, University of Virginia, 102 Engineer's Way, PO Box 400741, Charlottesville, VA 22904-4741, USA. Tel.: +1 4349246284; fax: +1 4349822658.
E-mail address: rjd4f@virginia.edu (R.J. Davis).

http://dx.doi.org/10.1016/j.apcata.2015.01.032
0926-860X/

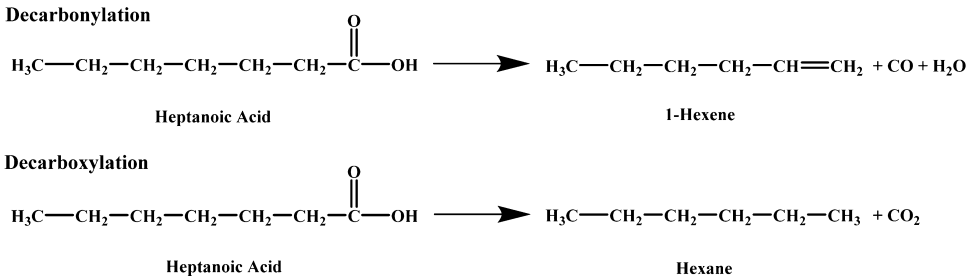

Scheme 1. Decarbonylation and decarboxylation of heptanoic acid.

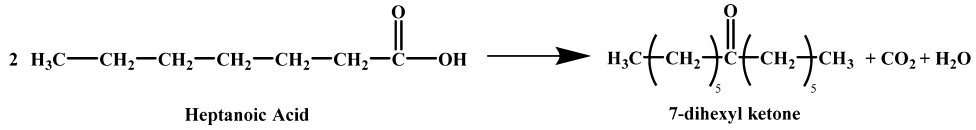

Scheme 2. Ketonization of heptanoic acid.

reported an increase in TOF by a factor of ≈32 when Pd nanoparticles were supported on silica instead of carbon [6], but Ford et al. reported a decrease in TOF of ≈3 fold when Pd nanoparticles were supported on silica instead of carbon during the liquid-phase operation [22]. In a different study, Lugo-José et al. reported during the gas-phase deoxygenation of propanoic acid at 473 K a constant TOF over Pd nanoparticles with sizes between 3.0 and 12 nm, but the TOF decreased by a factor of 3 when Pd nanoparticles of 1.9 nm were used instead [7]. In contrast, Simakova et al. reported an increase in TOF as the Pd nanoparticle size decreased from 6.1 to 2.3 nm during the liquid-phase deoxygenation of palmitic and stearic acid at 573 K [19].

Given the diversity of results reported for the conversion of carboxylic acids over supported Pd catalysts, which seem to depend on both catalyst type and reaction conditions, we studied systematically the decarbonylation and decarboxylation of heptanoic acid over a wide variety of supported Pd catalysts in a continuous-flow fixed-bed reactor. This study highlights the effect of reaction conditions on catalyst stability and reactivity. In particular, the effects of support type, Pd impregnation method, Pd weight loading, acid conversion, reaction phase, and acid concentration on the activity, product selectivity, and catalyst stability were examined.

2. Experimental methods

2.1. Catalyst synthesis

The catalysts were prepared by incipient wetness impregnation (IWI) using aqueous solutions of tetraamminepalladium (II) nitrate, $(NH_3)_4Pd(NO_3)_2$ (Sigma–Aldrich) to obtain 1, 5, 10, and 20 wt% Pd loadings on Norit activated carbon (ROX 0.9), respectively. Prior to impregnation, Norit carbon particles were crushed and sieved between 180 and 425 μm. After impregnation of the desired metal precursor solution, the catalyst was dried in air at 393 K overnight. Palladium (II) acetate, $Pd(OCOCH_3)_2$, was used to prepare catalysts by the alcohol reduction (AR) method, as described by Benavidez et al. [27], to obtain a 5 wt% loading on Norit activated carbon, Vulcan carbon (XC-72), and Davisil silica 636. Vulcan carbon and Davisil silica were used as received. All of the dried solids were reduced in H_2 (GTS-Welco 99.999%) flowing at 100 $cm^3\ min^{-1}$. The temperature of reduction was increased at 1 K min^{-1} from room temperature to 623 K, and held isothermally for 3 h. The catalysts were then cooled, exposed to air, and stored in a vial.

2.2. Dihydrogen chemisorption

The Pd dispersion was measured by H_2 chemisorption performed on a Micromeritics ASAP 2020 system. Each catalyst was evacuated at 573 K for 10 h under vacuum followed by heating to 623 K at a rate of 1 K min^{-1} after which it was reduced with flowing H_2 (GTS-Welco 99.999%) at 623 K for 3 h. Following reduction, the catalyst sample was evacuated at 573 K and cooled in vacuum to 373 K to prevent β-phase hydride formation during chemisorption. The amount of metal on the surface was evaluated by the total amount of H_2 adsorbed extrapolated to zero pressure, assuming a stoichiometric relationship between H_2 to metal of 1:2 (i.e. H/Pd = 1). The average spherical Pd particle size from chemisorption, which is analogous to the surface-weighted average Pd particle size [28], was estimated from the inverse of the Pd dispersion (i.e. inverse of the fraction of metal exposed) [29].

2.3. Dinitrogen physisorption

The specific surface area and pore size were measured by N_2 physisorption using a Micromeritics ASAP 2020. The samples were evacuated for 180 min at 373 K prior to the N_2 physisorption, after which adsorption isotherms were measured at 77 K. The Brunauer–Emmett–Teller (BET) and the Barrett–Joyner–Halenda (BJH) methods were used to determine the specific surface area and the pore size, respectively.

2.4. X-ray diffraction

Powder X-ray diffraction (XRD) analysis from $2\theta = 20$ to 100° was carried out on a X'Pert Pro MPD with monochromatic Cu Kα-radiation using a step size of 0.05°. The Scherrer analysis [30] was used to determine the average Pd crystallite size according to Eq. (1):

$$D_{\text{Pd Crystallite}} = \frac{\kappa\lambda}{\beta\cos\theta} \quad (1)$$

where $D_{\text{Pd Crystallite}}$ represents an average Pd crystallite size analogous to the volume-weighted apparent Pd crystallite size [28], κ represents the shape factor (e.g. 0.9 for this case), λ represents the X-ray wavelength (1.54056 Å for the Cu Kα-radiation), β represents the full width at half maximum (FWHM) of a specific diffraction peak, and θ represents the diffraction angle. Using the JADE 2010 software, we did a profile fit to all of the Pd diffraction peaks, and the average Pd crystallite size was determined over multiple peaks.

Please cite this article in press as: J.A. Lopez-Ruiz, et al., Appl. Catal. A: Gen. (2015), http://dx.doi.org/10.1016/j.apcata.2015.01.032